IOP Conf. Series: Materials Science and Engineering **739** (2020) 012036 doi:10.1088/1757-899X/739/1/012036

Numerical Simulation and Experiment of a MEMS Ultrasonic Cavitation Model

Zihong Liu[1, 2, 3], Hui You[1, 3*], Liangchao Li [2], Ronghui Lin[1], Ping Zhang[1]

[1]Department of Precision Instrumentation and Machinery, University of Science and Technology of China, Hefei 230026, Anhui, China
[2]Key Laboratory of Testing Technology for Manufacturing Process of Ministry of Education, Southwest University of Science and Technology, Mianyang 621010, Sichuan, China
[3]Institute of Intelligent Machines, Chinese Academy of Science, Hefei 230031, Anhui, China

usmlhy@iim.ac.cn

Abstract. This paper aims at analyzing the microbubble ultrasonic cavitation from the designed Bowl-shaped piezoelectric transducer in a micro channel. The cavitation conditions were derived and three methods of analysis were employed: (i) numerical analysis of piezoelectric parameters for the bubble cavitation using 2D piezo-acoustic coupling modelling. (ii) numerical analysis of microbubble dynamics and activities under ultrasound irradiation using 2D CFD simulation. (iii) experimental analysis of ultrasonic cavitation using designed micro-fluid chip by acoustic chemistry method. With the cavitation condition, the cavitation phenomenon of a lone micro bubble was analysed by the classic mathematical modelling, by which the piezoelectric transducer was optimized for ultrasonic cavitation in the micro channel. From the CFD results, the velocity of acoustic streaming increased to 58.6m/s, and the movement of the bubble wall was affected by the ultrasonic characters, which was in good agreement with the literature. The ultrasonic cavitation was proved to exist in the micro channel by the acoustic chemistry experiment.

1. Introduction

Cavitation [1, 2] is used to increase transiently the cell membrane permeability [3, 4] during exposure to ultrasound. The efficiency of the sonoporation is enhanced by the microbubble cavitation [5-7], which is a potential method used for gene delivery and drug delivery. The microbubbles are useful for improving the efficiency of the vivo sonoporation [8]. And the mechanisms of sonoporation caused by microbubbles has been revealed [9-12], the cell perforation and repair have been studied [13, 14]. However, most of the previous researches were carried out either in macro volumes with conventional ultrasonic equipment or in micro experiment model; there have been few studies on a Micro-Electro-[Mechanical-System(MEMS) device promising lab-on-chip approach to ultrasonic plasmid or DNA delivery, and the numerical analysis with the bubbles cavitation in the micro channel of the lab-on-chip device has not been elucidated.

To elucidate the mechanisms and the effect of the device parameters on the ultrasonic cavitation in the micro channel, we studied a MEMS device. In the micro channel, the core element of the MEMS device is a MEMS ultrasound transducer, which is designed to be a Bowl-shaped ZnO thin film structure to obtain a strong focusing effect. To analytically proof the feasibility of ultrasonic cavitation in the micro channel, the necessary and sufficient condition of the ultrasonic cavitation was deduced by using Blake threshold pressure and the Keller-Miksis equation [15]. For the necessary and sufficient condition of ultrasonic cavitation, the optimized geometric and physical parameters of the ultrasonic transducer was determined by simulated analysis using multiphysics soft COMSOL 5.3.

In the numerical simulation of the ultrasonic cavitation, it is assumed that there is a full-compressible gas dynamic in the bubble, the motion of the bubble wall was described by the Navier-Stokes equation and continuity equation in the micro-fluid channel. The boundary conditions near the moving bubble wall in the micro channel was set according to Rayleigh-Plesset equation and fluid-structure interaction in CFD simulation.

According to the optimized parameters and the analysis of the numerical simulation, the MEMS device was manufactured, on which the ultrasonic cavitation was proved to exist in the micro channel by acoustic chemistry experiment.

2. Methodology

2.1. Experimental model

Figure 1 shows the MEMS cavitation model, which utilizes ultrasonic cavitation to form reversible porosity in cell membrane for plasmid or DNA drug transfer. The core element of the system is a concave sphericity(Bowl-shaped) piezoelectric ultrasound transducer situated on bottom of the micro channel. The cross-sectional dimensions of the micro channel are 400um*400um.

In the cavitation experiment, the given solution is delivered into the micro channel by a peristaltic pump, and is collected by a collector. The micro bubble in the solution grows and compresses following the ultrasound in the micro channel. And the cavitation comes out as the micro bubble stored enough energy when compressed small enough.

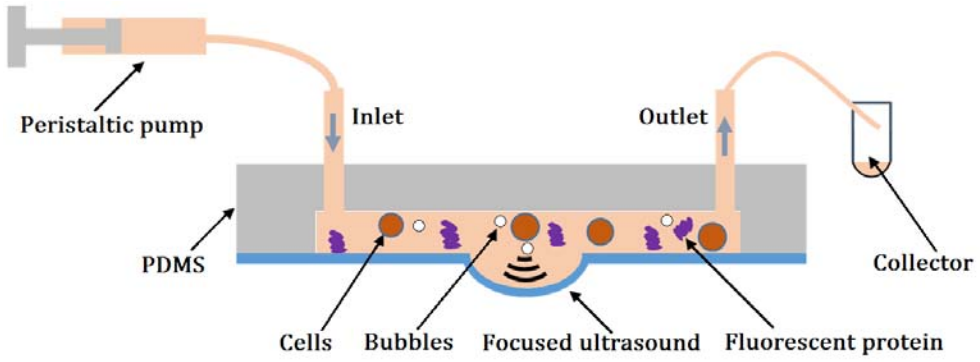

Figure 1. The cavitation experimental model of a micro-fluid system.

2.2. Mechanistical modeling base

According to the van der Waals equation [16], the pressure in or out the micro bubble is equal when the bubble is in equilibrium.

$$P_V + P_g\left(\frac{R_0}{R}\right)^3 = P_h + \frac{2\sigma}{R} \qquad (1)$$

Where, P_V is the vapour pressure in the bubble, P_g is the gas pressure in the bubble, P_h is the fluid pressure near the bubble, and σ is the coefficient of surface tension. The critical radius of the bubble in equilibrium is obtained by taking the derivative of the R in equation (1). The critical pressure P_k of the fluid near the bubble is given by bringing the critical radius into equation (1):

$$P_k = P_V - \frac{2}{3}\left[\frac{\left(\frac{2\sigma}{R_0}\right)^3}{3P_g}\right]^{\frac{1}{2}} \tag{2}$$

By taking $R = R_0$ and $P_V = 0$, P_k is calculated through equation (1) and equation (2):

$$P_k = -\frac{2}{3}\left[\frac{\left(\frac{2\sigma}{R_0}\right)^3}{3(P_h + \frac{2\sigma}{R_0})}\right]^{\frac{1}{2}} \tag{3}$$

P_k is negative in equation (3), which means that the negative pressure acting on the bubble is necessary for generating the bubble with initial radius R_0. Make $P_k = P_h - P_B$, the Blake threshold pressure P_B is defined by equation (3):

$$P_B = P_h + \frac{2}{3}\left[\frac{\left(\frac{2\sigma}{R_0}\right)^3}{3(P_h + \frac{2\sigma}{R_0})}\right]^{\frac{1}{2}} \tag{4}$$

In the study, the radial dynamics of the micro bubble was described by the Keller-Miksis equation. In this model, liquid compressibility and radiation dumping were considered through the time derivative of gas pressure [16]:

$$\frac{P_V + P_g\left(\frac{R_0}{R}\right)^3 - P_h'}{\rho} = R\frac{d^2R}{dt^2} + \frac{3}{2}\left(\frac{dR}{dt}\right)^2 + \frac{4\mu}{R}\frac{dR}{dt} + \frac{2\sigma}{\rho R} \tag{5}$$

In this equation, P_h', ρ and μ denote fluid pressure near the bubble wall, fluid density and shear viscosity of the fluid, respectively. Considering the effect of the ultrasound in the fluid, $P_h'(=P_h - P_a)$ is depended on the static pressure (P_h) and the ultrasonic pressure (P_a). where, $P_a(=-P_A\sin(\omega t))$ is determined by the acoustic pressure amplitude P_A and the acoustic pressure frequency $f(=\frac{\omega}{2\pi})$.

When ignoring the shear viscosity of the fluid, equation (5) is denoted:

$$R\frac{d^2R}{dt^2}+\frac{3}{2}\left(\frac{dR}{dt}\right)^2=\frac{1}{\rho}\left[\left(P_h+\frac{2\sigma}{R_0}\right)\left(\frac{R_0}{R}\right)^3-\frac{2\sigma}{R_0}-P_h+P_A\sin\omega_a t\right] \quad (6)$$

The equation (6) is expended to the $\frac{1}{R_0}$ power when the radial of the micro bubble is R ($=R_0+r,\ r<R$):

$$r^2+{\omega_r}^2 r=\frac{P_A}{\rho R_0}\sin\omega_a t \quad (7)$$

Where, ω_r ($=2\pi f_r$) is the resonance frequency. The normal resonance frequency (f_r) was given by Minneart according to equation 7[17]:

$$f_r=\frac{1}{2\pi R_0{}^2}\left[\frac{3}{\rho}\left(P_h+\frac{2\sigma}{R_0}\right)\right]^{\frac{1}{2}} \quad (8)$$

The cavitation is obvious when the ultrasonic frequency (f_a) is equal to f_r. The change in radial could be obtained by equation 7:

$$r=\frac{P_A}{\rho R_0\left({\omega_r}^2-{\omega_a}^2\right)}\left(\sin\omega_a t-\frac{\omega_a}{\omega_r}\sin\omega_r t\right) \quad (9)$$

According to equation 9 and equation 3, for smaller bubble, the bubble could collapse as $f_a < f_r$ and $P_A > P_B$.

2.3. Computational Fluid Dynamic

2.3.1. Ultrasonic in the micro fluid. Figure 2 shows the 2D geometric model of the axially symmetrical micro channel, in which the cross section of the channel is extended to 1000um*400um for numerical analysis of geometry parameters. The piezoelectric domain is made of the crystal ZnO, which is a common material in MEMS piezoelectric transducers. An AC electric potential of 100V is applied to the inside of the of the Bowl-shaped, while the outside is grounded. At the interface between the water and piezoelectric domain, the boundary condition for the acoustics interface is that the pressure is equal to the normal acceleration of the piezoelectric domain:

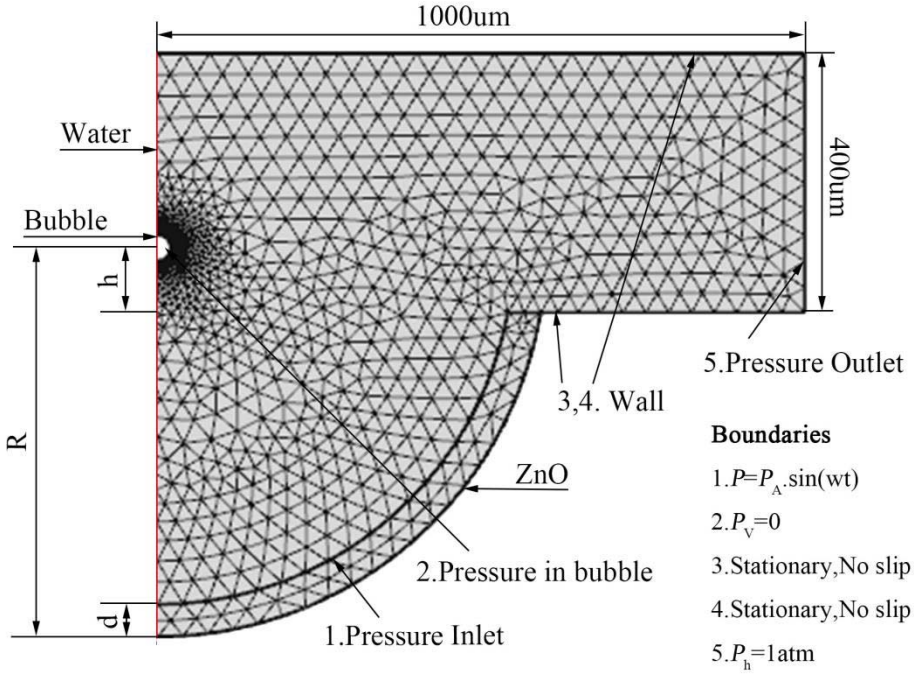

Figure 2. Geometric model used for ultrasound and bubble in the micro fluid.

$$\mathbf{n}\cdot\left(\frac{1}{\rho}(\nabla p)\right)=\mathbf{a_n} \tag{10}$$

Because there are no sources present, the wave equation in the water domain simplifies to:

$$\nabla\cdot\left(-\frac{1}{\rho}(\nabla p)\right)-\frac{\omega^2 p}{\rho c^2}=0 \tag{11}$$

Where c , $\mathbf{n}$ and $\mathbf{a_n}$ denote the velocity of sound in water, the normal vector, and the normal acceleration of the piezoelectric transducer. The ultrasonic pressure in the water could be obtained by Eq. equation (10) and equation (11), which changes in sine.

2.3.2. Micro-bubble dynamic. Since the flow rate in the micro channels is very low, it is assumed that the intensity of the sound field is constant, and the liquid in the micro channels is a kind of incompressible continuous media under normal temperature.

In the microfluidic channel, the motion of the bubble wall could be solved by the continuity equation and Navier-Stokes equation with the above governing equations.

Continuity equation:

$$\frac{\partial\rho}{\partial t}+\nabla(\rho\cdot\mathbf{u})=0 \tag{12}$$

Navier-Stokes equation：

$$\rho\frac{\partial \mathbf{u}}{\partial t}+\rho(\mathbf{u}\cdot\nabla)\mathbf{u}=\nabla\cdot[-p+\mu\left(\nabla\mathbf{u}+(\nabla\mathbf{u})^{T}\right)-\frac{2}{3}\mu(\nabla\cdot\mathbf{u})]+F \tag{13}$$

In this equation, F is the interfacial momentum. In this model (figure 2), the interface pressure between the piezoelectric transducer and water is:

$$p=p_h-P_A\sin(2\pi ft) \tag{14}$$

Where, P_h is the fluid pressure(=1 atm), and the ultrasonic pressure($=P_A\sin(2\pi ft)$) is obtained by equation (10). P_A and f refer to the ultrasonic amplitude and frequency. By taking the equation (14) into equation (13), the velocity of the bubble wall could acquire by equation (13) and equation (14).

2.3.3. Geometry, boundary conditions and numerical solution of equations. Equation (10) - (14) were numerically solved by COMSOL Multiphysics (Version 5.3). Figure.2 shows the geometric model and All details of the boundary, which is symmetrical. The residuals for all predicted parameters were considered to be less than 10-3. Furthermore, 189 boundary elements and 2416 region elements with minimum element quality of 0.0412um were considered. The Acoustic-Piezoelectric Interaction(acpz) and the Fluid-Structure Interaction(FSI), which are based on the Finite Difference Method(FDM), were used to solve the governing equations and the boundary [18].

3. Results and discussion

3.1. Geometry parameters of the acpz model

According to equation (4), Blake threshold pressure was P_B ($=1.1026\times10^5 P_a$) with the initial bubble radius R_0 (=4um) when the constant P_h ($=1.013\times10^5 P_a$) and σ ($=0.076 Nm^{-1}$) were determinate, which was greater than actual value. P_B was far below the gasification pressure of the liquid, which was conducive to the formation of bubble nuclei and could cause instantaneous cavitation. The bubble location h(=0.1mm) in figure 2 was set for numerical comparison.

Figure 3 shows ultrasound pressure distribution on the axis of Bowl piezoelectric model and plate piezoelectric model. The ultrasonic pressure produced from Bowl is about 1.5 times bigger than the pressure from Plane with same conditions, which are both greater than P_B in the micro channel when the ultrasonic frequency is equal to the resonance frequency of the bubble. According to the cavitation condition mentioned above, bigger ultrasonic pressure is necessary for cavitation, and the Bowl piezoelectric ultrasonic transducer is designed. In the numerical analysis of Acoustic-Piezoelectric Interaction(acpz) model, the width of micro channel in the axis is designed to 4mm without distortion for two ultrasonic periods.

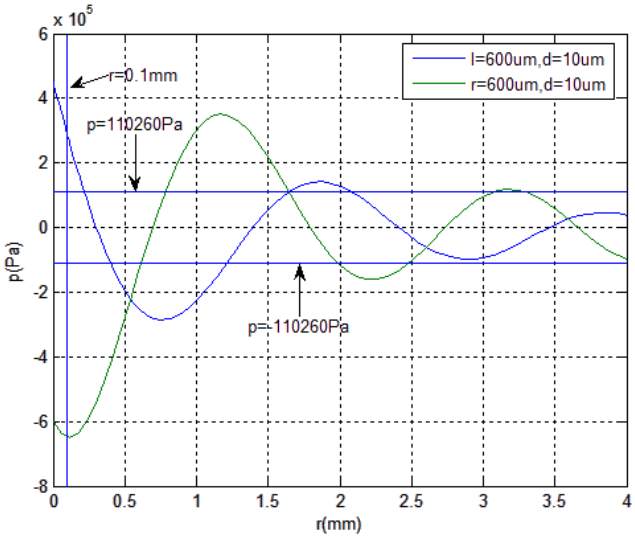

Green line(Bowl): h=0.1mm, r=0.6mm, d=0.01mm.
Blue line(Plane): h=0.1mm, l=0.6mm (equal to chord length of Bowl), d=0.01mm.

Figure 3. Axial acoustic pressure distribution from Bowl or Plate piezoelectric model.

Figure 3 shows that the amplitude of the axial ultrasonic pressure is bigger than Blake threshold P_B in the micro channel. In particular, the amplitude is about 6 times bigger than P_B in the location(h=0.1mm) of the bubble as blue line shown in figure 3.

Figure.4 shows ultrasound pressure distribution on the axis with different piezoelectric thickness d, arc chord distance h and radius r of the Bowl piezoelectric ultrasonic transducer. d is inversely proportional to the axial ultrasonic pressure (figure 4 a). h and r are proportional to the axial ultrasonic pressure (figure.4 b, figure.4 c).

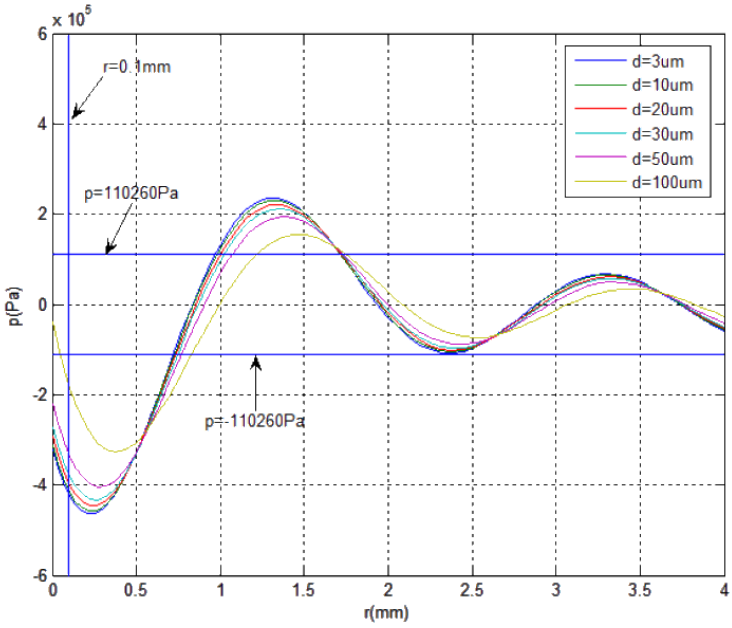

(a)

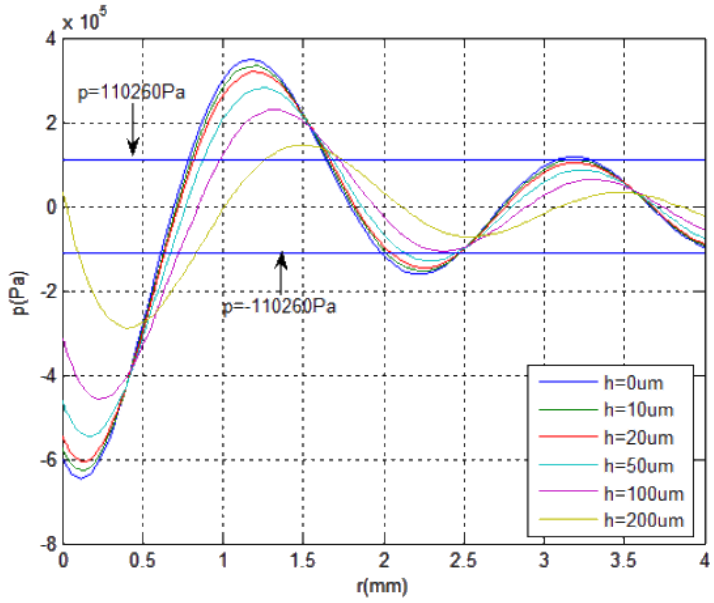

(b)

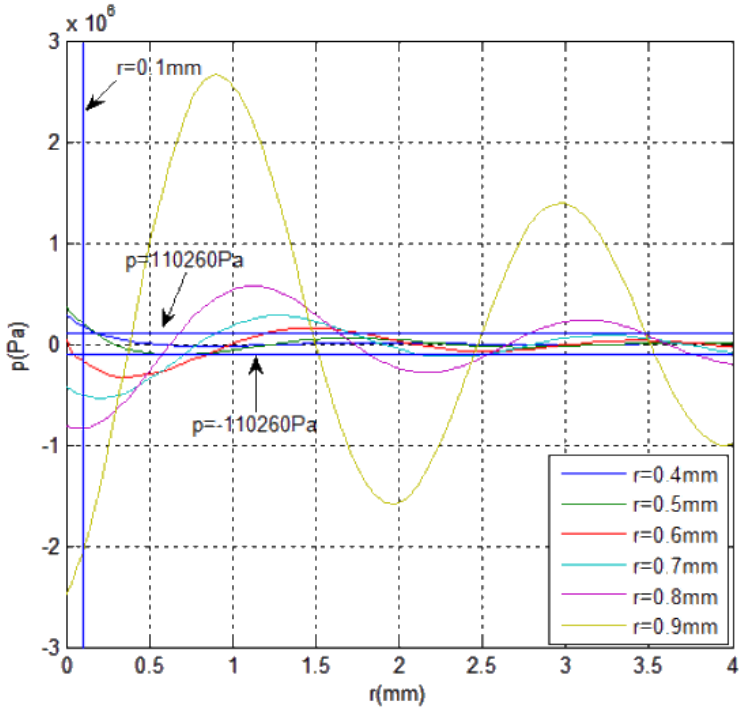

(c)

(a) h=0.1mm, r=0.6mm. (b) r=0.6mm, d=0.01mm. (c)h=0.1mm, d=0.01mm.

Figure 4. The axial ultrasonic pressure distribution with different transducer geometry parameters.

3.2. Micro bubble dynamics and activities under ultrasound irradiation

As acpz model mentioned above, the bubble (R=4um) was put to the sphere center of Bowl transducer in the FSI model. In order to better observe the bubble dynamics, the size of micro channel was reduced to 0.1 times without changing the ultrasonic and fluid characteristics around the bubble.

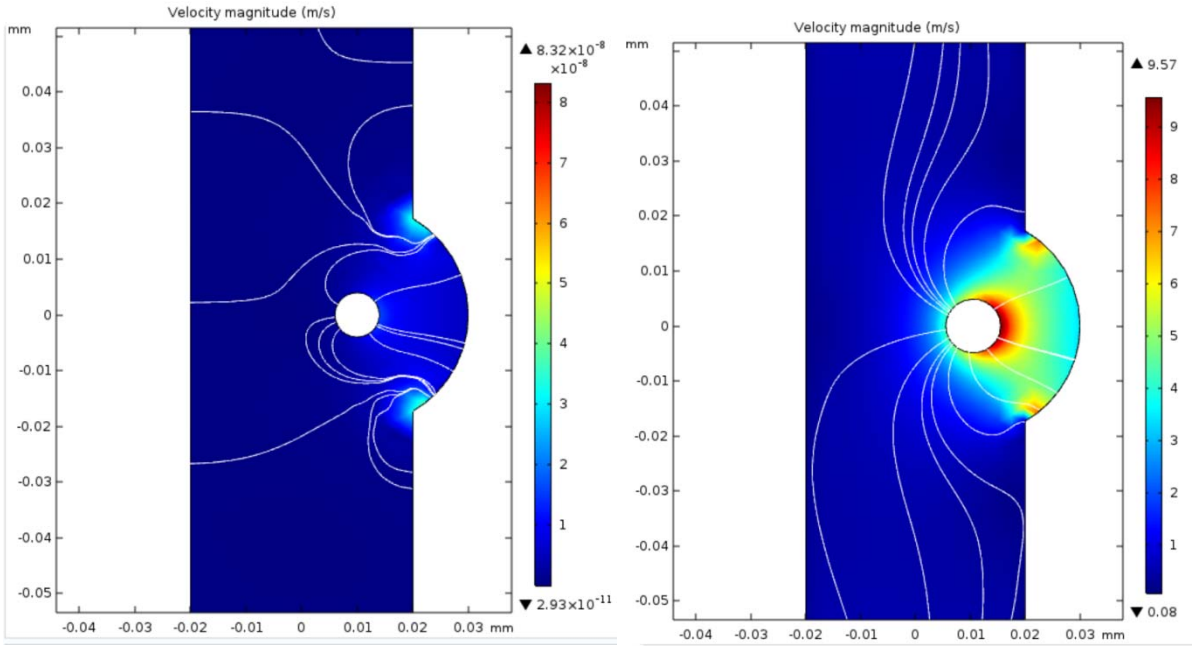

(a)

(b)

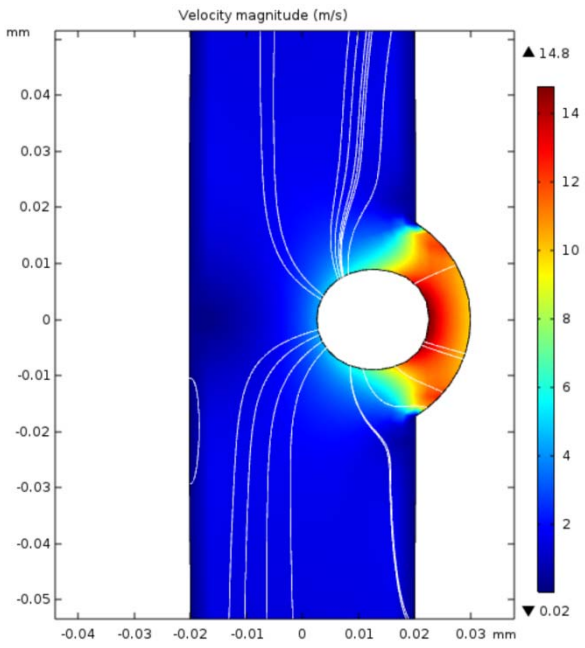

(c)

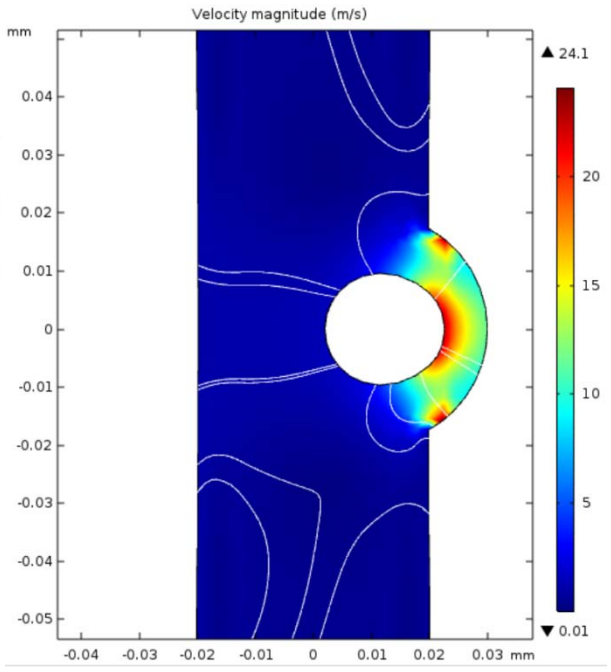

(d)

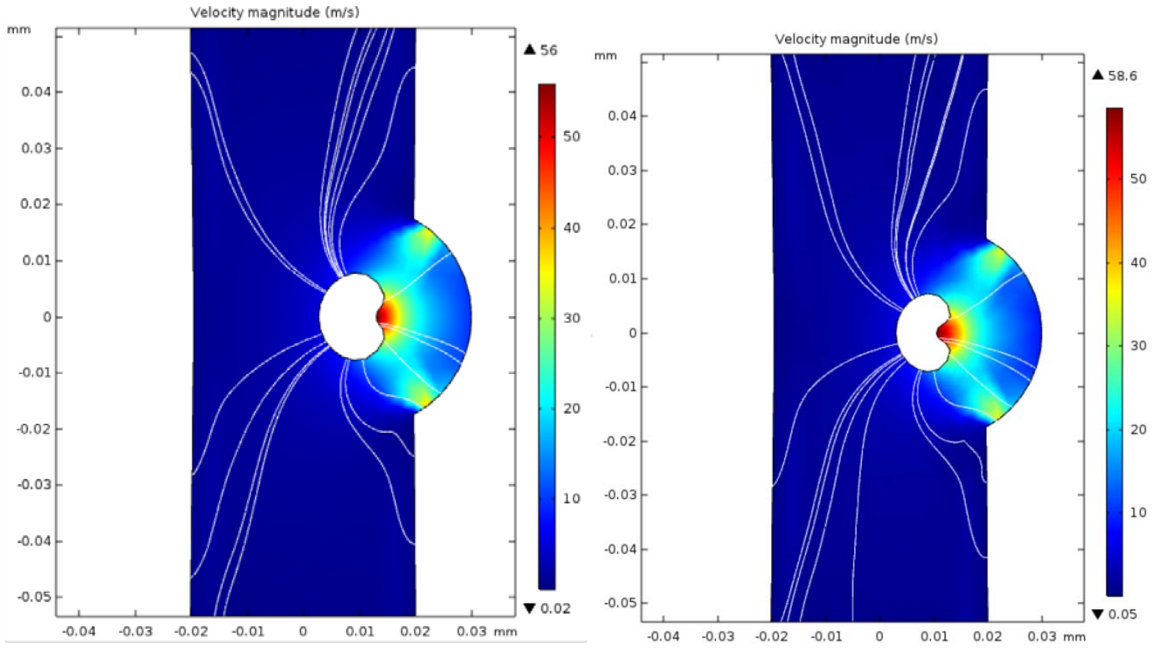

(e) (f)

(a) t=0. (b) t=0.25T. (c) t=0.5T. (d) t=0.75T. (e) t=0.875T. (f) t=0.89T

Figure 5. Micro bubble dynamics and activities under ultrasound irradiation.

Figure 5 shows the micro bubble dynamics and activities under ultrasound irradiation. It was observed that the bubble grew to the largest at 0.5T (T is ultrasonic period), and the invagination appeared near the side of piezoelectric transducer at 0.75T. The mesh of bubble wall collapsed at moment after 0.89T, and cavitation generated. The dynamics and activities of the micro bubble were consistent with the literature [19, 20]. According to equation (6), the radial dynamics of the micro bubble is highly consistent with figure.5, which confirmed the formation of cavitation in the micro channel.

3.3. The MEMS system and experiment

Figure 6 shows the experiment system [21]. In the micro-fluid experiment, the MEMS system is constituted of ultrasound transducer and micro channel. The substrate of the ultrasound transducer is the concave polyimide, which is made by a precision steel ball using embossing method. The piezoelectric thin film on the substrate is made by ZnO magnetron sputtering, on which two layers of Al are respectively electrodeposited as the positive electrode and negative electrode of the transducer. And the micro channels are made through soft imprinting method using polydimethylsiloxane(PDMS).

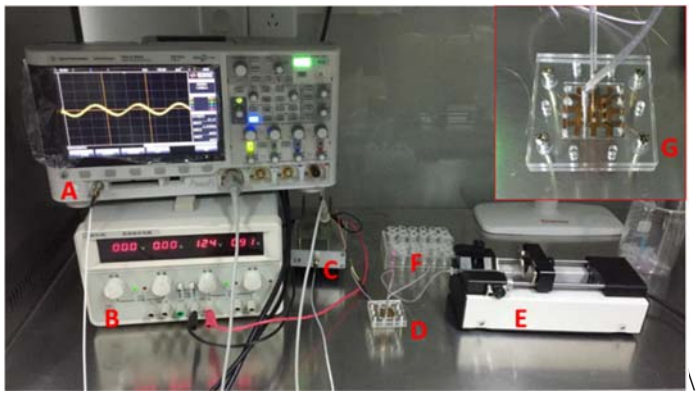

A. oscilloscope. B. stabilized voltage supply. C. power amplifier circuit.
D. microfluidic chip. E. peristaltic pump. F. collector. G. enlarge figure of microfuidic chip.

Figure 6. The experiment system of MEMS ultrasonic fluid system.

In the cavitation experiment, the hydroxyl terephthalic acid ions (HTA) has the characteristics of high fluorescence and stable chemical properties, by which the ultrasonic cavitation efficiency could be marked [22]. Figure 7 shows the relationship between fluorescence intensity of HTA (the solution is 8.0×10^{-3}mol/L) and the ultrasonic cavitations efficiency, which is tested by repeated experiment with the MEMS system (figure 6). Through a number of experiments, it is shown that the cavitation is generated in the liquid, and the ultrasonic cavitation is proportional to the fluorescence intensity.

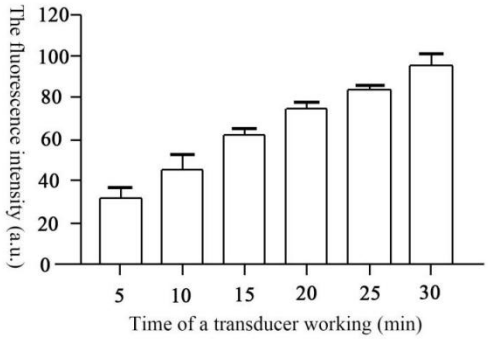

Figure 7. Ultrasonic cavitation experiment of MEMS transducer in the micro channels [23].

4. Conclusion

In the present study, the geometric parameters of the Bowl-shaped piezoelectric transducer are optimized according to the derived cavitation conditions, micro bubble dynamics and activities under ultrasonic irradiation was analyzed by CFD simulation, and ultrasonic cavitation is proved to exist in the MEMS chip by a number of acoustic chemistry experiments.

The axial ultrasonic pressure is inversely proportional to thickness d, proportional to arc chord distance h and radius r of the Bowl-shaped piezoelectric ultrasonic transducer, and the amplitude of the ultrasonic pressure in the circle center of the transducer is about 6 times bigger than Blake threshold pressure with designed geometric parameters (h=0.1mm, r=0.6mm, d=0.01mm). The concave of the bubble wall appeared near the side of piezoelectric transducer, and the velocity of acoustic streaming increased to 58.6 m/s in the concave area according to the CFD simulation result. Dynamics and activities of the bubble were in great agreement with the literature [19, 20].

Acknowledgements
The authors are grateful for the support provided by National Natural Science Foundation of China (Grant No.61176105), and Sichuan Education Department Program, China (Grant No.14ZB0112).

References
[1] Young F. R 1999 Cavitation *World Scientific.*
[2] Leighton T 2012 The Acoustic Bubble *Academic Press.*
[3] Newman C. M, Lawrie A, Brisken A. F and Cumberland D. C 2001 Ultrasound gene therapy: on the road from concept to reality *Echocardiog.* **18(4)** 339-47.
[4] Bao S, Thrall B. D and Miller D. L 1997 Transfection of a reporter plasmid into cultured cells by sonoporation in vitro *Ultrasound Med. Biol*. **23(6)** 953-9.
[5] Nobuki K, Okada K and Yamamoto K 2009 Sonoporation by Single-Shot Pulsed Ultrasound with Microbubbles Adjacent to Cells *Biophysical J*. **96(12)** 4866-76.
[6] Greenleaf W. J, Bolander M. E, Sarkar G, Goldring M. B and Greenleaf J. F 1998 Artificial cavitation nuclei significantly enhance acoustically induced cell transfection *Ultrasound Med. Biol.* **24(4)** 587-95.
[7] Lawrie A, Brisken A. F, Francis S. E, Cumberland D. C, Crossman D. C, Newman C. M 2000 Microbubble-enhanced ultrasound for vascular gene delivery *Gene Therapy*. **7(23)** 2023-27.
[8] Taniyama Y, Tachibana K, Hiraoka K, Namba T, Yamasaki K, et al. 2002 Local delivery of plasmid DNA into rat carotid artery using ultrasound *Circulation* **105(10)** 1233-9.
[9] Ohl C. D and Ikink R 2003 Shock-wave-induced jetting of micron-size bubbles *Phys. Rev. Lett.* **90(21)** 204502.
[10] Postema M, Van Wamel A, Lancee C. T and De Jong N 2004 Ultrasound-induced encapsulated microbubble phenomena *Ultrasound Med. Biol.* **30(6)** 827-40.
[11] Okaka K, Kudo N, Niwa K and Yamamoto K 2005 A basic study on sonoporation with microbubbles exposed to pulsed ultrasound *J. Med. Ultrasonics*. **32(1)** 3-11.
[12] Prentice P, Cuschieri A, Dholakia K, Prausnitz, M and Campbell P 2005 Membrane disruption by optically controlled microbubble cavitation *Nat. Phys*. **1(2)** 107-10.
[13] Kudo N, Okada K and Yamamoto K 2009 Sonoporation by Single-Shot Pulsed Ultrasound with Microbubbles Adjacent to Cells *Biophys. J*. **96(12)** 4866-76.
[14] Deng C. X, Sieling F, Pan, H and Cui J 2004 Ultrasound-induced cell membrane porosity *Ultrasound Med. Biol.* **30(4)** 519-26.
[15] Leighton T. G 2007 Derivation of the Rayleigh-Plesset Equation in Terms of Volume *University of Southampton.*
[16] Lofstedt R, Weninger K, Puterman S, Barber B. P 1995 Sonoluminescing bubbles and mass diffusion *Phys. Rev. E* **51(5)** 4400.
[17] M.Minneart, Philos.Mag.16(1933) 235.
[18] Sajjadi B, Raman A. A. A, Ibrahim S and Shah R. S. S. R. E 2012 Review on gas liquid mixing analysis in multiscale stirred vessel using CFD *Rev. Chem. Eng*. **28** 171-89.
[19] Kudo N, Okada K, Yamamoto K 2009 Sonoporation by single-shot pulsed ultrasound with microbubbles adjacent to cells *Biophys. J*. **96(12)** 4866-76.
[20] Blake J. R, Taib B. B, Doherty G 1986 Transient cavities near boundaries. Part 1. Rigid boundary *J. Fluid Meechan*. **170** 479-97.
[21] Lin R 2016 Self-focused Piezoelectric Micromachined Ultrasonic Transducer and Its Application in Cell Delivery *Uni. Sci. Technol, China.*
[22] Mason T. J, Lorimer J. P, Bates D. M, Zhao Y 1994 Dosimetry in sonochemistry: the use of aqueous terephthalate ion as a fluorescence monitor *Ultrason. Sonochem.* **1(2)** S91-5.
[23] Zhang P 2016 Research on Gene Transfection by Ultrasound Method under the Microfluidic Environment *Uni. Sci. Technol, China.*